Silva, H. G., Conceição , R., Khan, A., Matthews, J., Wright, M., Collares-Pereira , M., & Shallcross, D. (2016). Atmospheric electricity as a proxy for air quality: Relationship between potential gradient and pollutant gases in an urban environment. *Journal of Electrostatics*, *84*, 32-41. https://doi.org/10.1016/j.elstat.2016.08.006

Atmospheric Electricity as a proxy for Air Quality: relationship between Potential Gradient and Pollutant Gases in an Urban Environment

H.G. Silva,[1*] R. Conceição,[1] M.A.H. Khan,[2] J.C. Matthews,[2] M.D. Wright,[2] M. Collares-Pereira,[1] D.E. Shallcross,[2]

[1]Renewable Energies Chair, University of Évora, IIFA, Palácio do Vimioso, Largo Marquês de Marialva, 7002-554, Évora, Portugal

[2]Atmospheric Chemistry Research Group, School of Chemistry, University of Bristol, Cantock's Close, Bristol, BS8 1TS, UK.

Keywords: Air Pollution, Trace Gases, Particulate Matter, Atmospheric Electric Potential Gradient

*Corresponding author:

Hugo Manuel Gonçalves da Silva

Renewable Energies Chair

University of Évora, IIFA

Palácio do Vimioso

7002-554 Évora, Portugal

E-mail: hgsilva@uevora.pt

Highlights

(1) Atmospheric Electric Potential Gradient recorded at Lisbon (Portugal): 1988-1990.

(2) Different wind sectors are compared, corresponding to different pollution sources.

(3) A model is developed for the relationship between Trace Gases and Potential Gradient.

(4) The fitting parameters show consistency with the model.

(5) Evidence that PG and TG are mediated by the presence of Particulate Matter.

Abstract

A relationship between Trace Gases (TG), NO_x, SO_2, O_3, and the Atmospheric Electric Potential Gradient (PG), through Ion/Particulate Matter (PM) interaction, is established in the urban environment of the city of Lisbon (Portugal). Analysis was restricted to 1988-1990, when simultaneous measurements of PG and TG were taken. Reasonable linear relationships between PG and TG concentrations have been found. A formulation relating PG with TG concentrations allows the estimation of constants of proportionally between TG-PM to be ~50 $cm^{-3}ppb^{-1}$; which are similar to the values found in direct TG-PM measurements in UK cities, validating the present results.

1. Introduction

Air pollution can be defined as the presence of pollutants, such as nitrogen oxides (NO_x), sulphur dioxide (SO_2), ozone (O_3), carbon monoxide (CO) and particulate matter (PM) in the air, which can cause negative effects on human health and vegetation (Fleming et al., 2005). Emissions of these pollutants can lead to a complex series of physical and chemical transformations in urban and regional areas (NRC, 1991). The main source of NO_x in an urban environment is fossil fuel combustion originating from both stationary sources (i.e. power generation) and mobile sources (i.e. transport), while minor natural sources can include bacteria, volcanic action and lightning and non-combustion anthropogenic processes (e.g. HNO_3 manufacture, welding processes and the use of explosives). The annual mean concentrations of NO_2 (the major component of NO_x) in urban areas are generally found to be between 20 and 90 μgm^{-3} (~10 to 48 ppb), with peaks occurring twice a day as a consequence of rush hour traffic (Niemelä et al., 2011). In urban areas, SO_2 is emitted predominantly from fossil fuel combustion at power plants, residential activities (e.g. heating), traffic, and other industrial facilities, as well as from shipping near ports and coastal or inland

shipping routes (Eyring et al., 2010). Other minor sources of SO_2 include smelting, manufacturing of sulphuric acid, conversion of wood pulp to paper, incineration of refuse and extraction of elemental sulphur from ore. The annual urban mean concentrations of SO_2 in Europe and the US oscillated between 10 to 30 μgm^{-3} (~3 to 12 ppb) (Möller, 2010). O_3 is an important photo-oxidant that is produced from NO_x catalysed photochemistry throughout the troposphere (e.g. Jenkin and Clemitshaw, 2000). Other photochemical reactions can produce a number of oxidants including peroxyacetyl nitrate as well as aldehydes, formic acid, and an array of short-lived radicals which can produce and build up O_3 downwind of urban areas. The maximum level of O_3 observed in urban areas is well above 100 ppb (e.g. Hanrahan, 2009). PM in urban areas is mainly composed of metals, organic compounds, materials of biological origin and elemental carbon (e.g. Tasic et al., 2006). Particulates can be classified as either primary or secondary, according to their origin. Primary particulates are those emitted directly to the atmosphere while secondary particulates are those formed by reactions involving other pollutants. In the urban context, most secondary PM occur as sulphates and nitrates formed from reactions involving SO_2 and NO_x, with typical annual mean values between 10-40 μgm^{-3} (black smoke method) or 50-150 μgm^{-3} (gravimetric method) (Shah et al., 1997). At the sub-micron fraction (PM_1), there is often a significant contribution from secondary organic aerosol (SOA) as highlighted by Lanz et al. (2010).

In atmospheric electricity a global electrical circuit is evidenced by a measurable atmospheric electric potential gradient at the Earth's surface, usually referred to as Potential Gradient (PG[1]). Global thunderstorm activity transfers charge to the ionosphere, which returns to the ground by means of an air-Earth current through air, which is weakly ionised due to the presence of cluster-ions produced by solar and cosmic rays and ground based radiation. PG typically has a magnitude between 100 and 200 Vm^{-1} in fair weather, but can be affected by sources of space charge, such as charged clouds or local sources of ions (Harrison, 2004). The effect of air pollutants, specifically particulate matter (PM), on the atmospheric PG is one of the most successful and largely explored applications of atmospheric electricity. Recent publications by the authors review this in detail; the interested reader is referred to these publications (Silva et al. 2014, Silva et al. 2015a, b). The basic physics of this process is summarized as follows: an increase in PM concentration depletes ions in the atmosphere, reducing the air conductivity and hence (according to Ohm's law) increases PG. Of particular interest has been the ability to use historical records of PG since the industrial revolution (Aplin, 2012) to retrieve pollution dynamics and smoke estimates (Harrison, 2006). More recently,

[1] PG is defined as the vertical component of the surface atmospheric electric field, E_z, by definition this field is negative in fair-weather days (field vector directed downwards). The convention used for PG, in order to have positive values for fair-weather days, is to define $PG=-E_z$. This definition has been used from the beginning of atmospheric electricity and details can be found at (Chalmers, 1967)

attention has been given to the possibility of assessing smoke plume dynamics by combining PG measurements with HYSPLIT particle trajectory modelling (Conceição et al., 2015).

To date, much less attention has been given to the relationship between Trace Gases (TG) and PG. In the literature the most prominent publications on this subject are those by Guo and co-authors, (Guo et al., 1996a, b). In these papers those authors state that PG can be simultaneously a proxy of both PM and TG; the argument given to justify this is that both TG and PM influence the PG, but according to different mechanisms. The linear relationship between PG and PM is well established and has been described earlier. In the case of TG, the linear influence on PG is justified as TG contribute to the increase of the ion recombination rate, α (Guo et al., 1996a, b). This results in a net reduction of ion production that consequently reduces the air conductivity and therefore increases PG; explaining the PG-TG relationship. A detailed discussion of ion recombination is beyond the scope of the present work, but the interested reader is referred to seminal works on atmospheric ions available in the literature, e.g. Anderson (1977). Furthermore, this mechanism has been intensively debated as ion recombination is considered to be a key aspect in particle formation (e.g. the CLOUD experiments at CERN, Kirkby et al., 2016 and references therein) but it is the current view that there is no direct relationship between TG concentration and PG. The observed statistical correlation for PG and TG found in the work of Guo and co-authors (Guo et al., 1996a, b) is considered to result from an indirect relation; TG are proportional to PM and as PM influences PG a relation appears to hold between PG and TG. Proportionality of TG and PM concentrations has been shown in a number of different studies undertaken in urban environments. Among which, Longley et al. (2005) analysed data from Manchester, Birmingham and Edinburgh (UK) and found reasonable values of proportionality, ~50 $cm^{-3}ppb^{-1}$, for PM and TG concentrations. Therefore, empirical evidence justifies the assumption of a linear relationship between TG concentrations and atmospheric PG measured at ground level.

The present work aims to clarify the linear relationship between PG and TG concentration, mediated by PM, as observed by Guo et al (1996a, b). A linear proportionality is assumed between PM and TG, following observations by Longley et al. (2005), and the formulation derived by Harrison (2006), is adapted to describe the linear relationship between PG and PM. With these assumptions a simple formula is derived for the PG-TG relationship which is shown to be linear. This formula is tested against observations in Lisbon, Portugal (1988-1990) and reasonable results are found which are supportive of the indirect PG-TG relation, clarifying this long-standing issue.

2. Theoretical background and formulation

The theoretical framework for the approach used here follows a similar method outlined in previous work by the authors (Silva et al. 2015a). Atmospheric small ions (clusters of molecules around a central ion) are produced by ionisation of air molecules, mainly by cosmic rays or radioactive decay (Harrison and Carslaw, 2003). A steady-state equation for ion formation and loss in the presence of PM was derived by Hoppel (1985) and is expressed as:

$$q - \alpha n^2 - \beta_a Z_a n = 0 (1)$$

Where $n$is the mean ion concentration, $q$is the ion production rate (this is assumed to be $q \sim 10\text{cm}^{-3}\text{s}^{-1}$), α is the ion recombination rate, β_a is the effective ion-PM attachment coefficient for the PM size distribution in question, and Z_a is PM number concentration. Eq. (1) neglects the positive to negative ion imbalance, as it is assumed a quasi-equilibrium state perturbed by the presence of PM. To relate urban PG measurements with TG, it is considered that most of the atmospheric ion loss is caused by ion-PM attachment and not by ion recombination; this assumption is validated by the work of Tammet et al. (2006). The solution to this equation is straightforward:

$$n = \frac{1}{2\alpha}\left[\sqrt{(\beta_a Z_a)^2 + 4\alpha q} - \beta_a Z_a\right]. (2)$$

For cases with relatively high PM concentration (~3000 cm^{-3}), such as would be expected in urban environments, Eq. (2) can be expanded in a Taylor series to yield a simple relationship between ion number concentration and PM number concentration:

$$n \approx \frac{q}{\beta_a Z_a}. (3)$$

Details of this derivation can be found in Silva et al. (2015a). With Eq. (3) the atmospheric electric conductivity can be written as:

$$\sigma_t = 2\mu_m e n \approx \frac{2\mu_m e q}{\beta_a Z_a}, (4)$$

where μ_m is the mean electric mobility (the factor 2 is justified by the contribution of both positive and negative ions having similar mobilities) and e is the electron charge. The influence of charged PM on atmospheric electric conductivity is neglected due to their relatively low mobility (Wright et al., 2014). Using (quasi-static) Ohm's law, it is possible to relate PG with σ_t by:

$$PG = \frac{J_z}{\sigma_t} \approx \frac{J_z}{2\mu_m eq} \beta_a Z_a, (5)$$

Where J_z is the air-Earth density current (usually considered to be ~2 pAm^{-2}). Eq. (5) relates PG and Z_a linearly and is similar to relationships found by Silva et al. (2015a), Harrison (2006) and Harrison and Aplin (2002). Finally, supported by experimental observations by Longley et al., (2005), an empirical linear relation is used to relate Z_a and TG concentration, $[X]$, of the type:

$$Z_a \approx Z_{0,X} + y_X[X], (6)$$

where y_X is the constant of proportionality between TG and the PM concentration (in units of cm^{-3} ppb^{-1}), $Z_{0,X}$ is the background PM constant, and X is the concentration of either NO_x, SO_2 or O_3. A linear relation between TG and PG can be deduced as:

$$PG \approx \frac{J_z \beta_a Z_{0,X}}{2\mu_m eq} + \frac{J_z \beta_a y_X}{2\mu_m eq}[X], (7)$$

Eq. (7) can be further modified by the use of Gunn's formula (Gunn, 1954), $\beta_a = 4\pi k_B T \mu_m e^{-1} R_a$, to yield:

$$PG \approx \frac{2\pi J_z k_B T R_a}{e^2 q} Z_{0,X} + \frac{2\pi J_z k_B T R_a}{e^2 q} y_X[X]. (8)$$

where k_B is the Boltzmann constant; T is the ambient temperature (set here as 293 K); R_a is the effective PM radius in the context of Hoppel's theory (Hoppel, 1985) which is assumed to be $R_a = 0.1$ μm. The formulation developed by (Hoppel, 1985) uses effective parameters to simplify the equation for ion balance in the presence of a more realistic aerosol size distribution. The parameters $Z_{0,X}$ and y_X are determined for each TG according to the procedure described later.

3. Data

3.1 Meteorology

The former Portuguese Institute of Meteorology (IM) took meteorological measurements at the same station as PG was recorded (Lisbon Airport, Portugal: 38°46'32''N, 9°07'30''W, Figure 1). The data used in the present study were retrieved from the NNDC Climate Data Online website supported by NOAA. Two meteorological parameters were used: manually observed current weather (MW), which are important as precipitation and snow perturb PG (PG values having MW in the range of 50-99, corresponding to "precipitation at the station at the time of observation", were excluded); and wind direction (WD), because the PG has been shown to be strongly modulated by the nature of sources downwind (Silva et al., 2015a, b). According to the procedure in those two studies, TG and PG measurements are divided into four wind sectors:

1) NW, $270^{o} \leq \theta \leq 360^{o}$;
2) NE, $0 \leq \theta \leq 90^{o}$;
3) SE, $90 \leq \theta \leq 180^{o}$;
4) SW, $180^{o} \leq \theta \leq 270^{o}$.

Using the Portela station as a geographic reference, the main pollution sources (e.g. industry and traffic) were present within the Southern sectors whilst scarcer in Northern sectors. Portela was located in the Northern outskirts of Lisbon during the 1980s. The Tagus River basin and the Iberian Peninsula are located within the Eastern sectors whereas the Western sector is covered by the Atlantic Ocean. Significant industrial complexes existed in the late 1980s in the South margin of the Tagus River (Setubal region). The prevailing winds in Lisbon come from the NW and result from the Iberian thermal depression (Silva et al., 2015a). If the *Rua de "O Século"* station where TG measurements were taken, is used as a geographic reference Northern winds would carry pollution from the city, predominantly traffic, and the Southern winds would carry pollution from the industries mentioned previously.

3.2 Potential Gradient

A Benndorf electrograph was coupled to a radioactive probe to equalize potential between the sensor and the air and to improve the time response of the electrograph. It was installed 1 m above the ground in a cement base at the Portela meteorological station and recorded PG. Its sensitivity was checked using an electronic electrometer with a standard voltage source between ± 200 V; the same calibration procedure was used in all periods of operation. The paper records of the electrograph were digitalized at a later date (Serrano, 2010). Further details about the dataset can be

found in (Silva et al., 2014; Conceição, et al., 2015; Silva et al., 2015a). In this study, data from 1988 to 1990 (restricted by the TG data) were used and values of PG between 0 and 300 V/m were selected; these values are indicative of fair-weather conditions (Chalmers, 1967). A detailed description of the WD dependence of the PG can be found in previous works (Silva et al., 2015a, b)

3.3. Trace Gases

The gas species, NO_x, SO_2, O_3, were measured in the air quality station located at *Rua de "O Século"* (Lisbon city centre, Portugal: 38º42'44''N, 9º08'51''W) supported by the Lisbon Regional Coordination and Development Commission (Figure 1). The air quality station was located around 8 km NE from Portela station where PG was recorded. Measurements began in 1988 but during most of that year, it was in a trial stage and the validated data available did not reach 75%, only validated data are used here. The operation of the station has continued (with several upgrades) to the present day, but only the years 1988 to 1990 are considered here as PG records end in 1990. NO_x, SO_2, and O_3 were measured by chemiluminescence (Environment AC 3OM), UV fluorescence, and ultraviolet absorption (Dasibi 1003 RS), respectively. Unfortunately, no reliable CO and PM measurements exist from this station. NO_x, SO_2 and O_3 were separated according to wind direction at the Portela station. The reason that wind directions at Portela were chosen instead of at *Rua de "O Século"* was because the main focus of the present work is to compare the PG measurements with the TG. However, if Lisbon climatology is taken into account, (Silva et al. 2014, 2015a), the winds in Portela can be considered as representative of those in the city centre.

4. Results and Discussion

TG concentrations are represented in histograms according to the wind sectors, defined previously, in Figure 2, it can be seen that NO_x, SO_2 and O_3 have similar distributions for each wind sector and their values occur predominantly in the 0 to 200 ppb range. Northern wind quadrants are more numerous than Southern quadrants as a result of the dominant Northern winds in Lisbon, the so-called *Nortada* regime (Silva et al., 2015a). The mean concentrations of NO_x, SO_2 and O_3 tend to be higher for Northern winds, especially NE, as compared with Southern ones, in particular SW (Table 1). Additional statistical parameters can also be found in Table 1. These are consistent with the fact that Northern winds carry higher NO_x and SO_2 concentrations than Southern ones, this implies that most of these two pollutants are generated by urban activity (mainly traffic) in the city instead of the industrial regions in the Southern wind sectors, which are known to be significant sources of PM (Silva et al., 2015a,b). Further evidence that this is the case is that the NE sector has the highest

mean values of the four sectors for both NO_x and SO_2. In *Rua de "O Século"*, NE winds are the most likely to carry air pollution from the city to the station and show a stronger relationship with PG, as will be shown later. The finding that Northern winds have higher concentrations of NO_x and SO_2 reinforces the importance of urban activity on the concentrations of these gases within the city centre. The NW sector has the highest concentrations of O_3 and the remaining wind sectors have similar values, this is likely to be due to the presence of *Serra de Monsanto*, Figure 1, a densely forested part of NW Lisbon and a source of volatile organic compounds (VOC) which can be responsible for the generation of O_3 through a positive feedback process described in detail in (Pinto et al., 2010) but noted in several studies elsewhere, where a large source of reactive VOCs exacerbates ozone production in the presence of significant NO_x emissions (e.g. Horowitz et al., 2007).

Lomb-Scargle periodograms (Scargle, 1982; Silva et al., 2014) for each of the three gases were calculated using the Bret Schoelson (2001) implementation and are presented in Figure 3. These periodograms indicate dominant cycles in uneven time-series, in this case these are the annual (1 year) and weekly (7 days) periods. A weekly periodicity is commonly attributed to anthropogenic action (Tchepel and Borrego, 2010) as during a working day there is a greater amount of human activity (predominantly traffic) producing more pollution than at weekends. For that reason, work days have higher TG concentrations than weekends causing a weekly periodicity. Therefore, the weekly cycle has been used as a proxy to infer an anthropogenic influence on PG (Silva et al., 2014); a stronger weekly cycle implies greater anthropogenic influence and with it more pollution. Figure 3 confirms a source with a strong weekly cycle prevailing in the Eastern wind sectors, NE and SE indicating more sources of pollution in that region in accordance with the previous statistical description. The weekly periodicity points towards traffic as the main source for these gas species (Silva et al., 2014). An annual cycle is generally present in all wind sectors for all three gas species, this cycle also appears in PG (Silva et al. 2014), and is attributable to seasonal meteorological variations imposing a strong modulation on TG. To further understand the dynamics of TG, boxplots representing the daily variation of their concentrations are shown in Figure 4. Both NO_x and SO_2 show two main peaks: one at ~8 UTC and another at ~18 UTC which correspond to rush hours in Lisbon and are consistent with the earlier finding that NE wind sectors show higher concentrations. O_3 shows a single peak around ~14 UTC (NW wind sectors show higher concentrations) which implies higher levels of photochemical activity due to the increase in solar radiation at mid solar day (McKee, 1994) that in Lisbon corresponds to ~14 UTC.

To identify the possible relationship between TG and PG three steps are taken. First, PG values are separated into TG concentration bins with a given width, $\Delta[X] = 10$ ppb, from $[X]_{ini} = 0$ ppb up to $[X]_{end} = 90$ ppb. The condition for each j-bin is:

$$[X]_{ini} + (j-1)\Delta[X] < [X](j) \leq [X]_{ini} + j\Delta[X], \quad (9)$$

The choice of $\Delta[X]$ has been made as a trade-off between the statistical representativeness of each bin and ensuring a sufficient number of values to enable statistical confidence in the analysis. Second, mean values (standard deviations are represented as error bars) of PG for each TG concentration bin have been calculated and are represented as a function of the mean value of the gas concentration for that bin, the results are shown in Figure 5. Third, Eq. (8) is used to fit the resulting values.

A good linear relationship between PG and TG is found in the four wind directions with goodness of fit, r^2, close to 1, the fitting parameters, $Z_{0,X}$ and y_X, are summarized in Table 2. Better fits (in terms of r^2) are found for the Northern wind sectors, NW and NE, for the three gas species and PG. The constants of proportionality for NW are found to be $y_{NO_x} = 27.38$ cm^{-3}ppb^{-1}, $y_{SO_2} = 45.73$ cm^{-3}ppb^{-1}, and $y_{O_3} = 35.14$ cm^{-3}ppb^{-1}. However, the values for NE are: $y_{NO_x} = 55.40$ cm^{-3}ppb^{-1}, $y_{SO_2} = 21.32$ cm^{-3}ppb^{-1}, and $y_{O_3} = 47.91$ cm^{-3}ppb^{-1}. Uncertainties in these parameters are < 0.01 cm^{-3} ppb^{-1} (a pessimistic evaluation was used). These are very similar to the values (~50 cm^{-3} ppb^{-1}) found by Longley et al. (2005) who measured CO, NO_x and PM number concentration in urban environments. Those authors undertook measurements in three busy UK cities, Manchester, Birmingham and Edinburgh, where road vehicle exhausts were the major sources of CO, NO_x and PM; similar to what happens in Lisbon. Actually, Lisbon in the 1980s was characterized by very heavy traffic that had (and still has) similarities with the urban environmental conditions of the three UK cities mentioned earlier. For that reason, it should be expected that a similar proportionality between PM and TG would be found in Lisbon. Nevertheless, finding this same proportionality between PM and TG in Lisbon as in the three UK cities by means of PG measurements is noteworthy and constitutes the most relevant result from the present study. It presents new possibilities in the use of PG measurements for air quality (in particular, PM) assessment in urban environments, and strengthens the points previously discussed in this context (Silva et al., 2014, 2015a).

It is important to highlight that NE winds tend to show a better r^2 in the relationship between PG and TG, this is tentatively explained by the fact that the NE winds include air transported from

Portela (where PG is measured) to *Rua de "O Século"* (where TG are measured) and for that reason a closer relationship between these variables is unsurprising. On the other hand, the background values of the PM number concentration, $Z_{0,X}$, seem to be higher for the Southern wind sectors than Northern sectors, and seem consistent with the results found previously by Silva et al. (2015a, b), as the main sources of PM would be likely to be present in the Southern part of the Tagus River where intense industrial activity existed in the 1980s. The presence of this source of pollution, which is substantially different from traffic, may also explain the weaker agreement (lower values of r^2) between PG and TG in following a linear relationship for the Southern winds, as PM and TG would have different sources and therefore a proportional relationship would no longer be expected. This assumption of proportionality is based on the indirect linear relationship of PG with TG, via PM, and if the proportionality does not hold, the PG-TG relationship also will not hold. It may also be due to a less favourable air transport from *Rua de "O Século"* (where TG are measured) to Portela (where PG is measured) and to a significantly lower number of recorded values (as confirmed by the number of hours, N.H., Table 1). The constants of proportionality for SE are found to be $y_{NO_x} = 82.61$ cm^{-3}ppb^{-1}, $y_{SO_2} = 21.77$ cm^{-3}ppb^{-1}, and $y_{O_3} = 59.53$ cm^{-3}ppb^{-1}. The values for SW are: $y_{NO_x} = 33.31$ cm^{-3}ppb^{-1}, $y_{SO_2} = 38.39$ cm^{-3}ppb^{-1}, and $y_{O_3} = 46.22$ cm^{-3}ppb^{-1}. Estimated errors are again < 0.01 cm^{-3} ppb^{-1}. Again these values are close to the values found by Longley et al. (2005) and provide a reasonable level of robustness in the use of PG measurements as a proxy of PM in urban environments.

To further evidence this, a scatter plot representation of SO_2 as a function of NO_x with the corresponding values of PG represented as a colour gradient is now presented in Figure 6. Scatter plots are frequently used in environmental sciences to understand the inter-relationship between three different atmospheric constituents, e.g. NO_x, O_3 and HCOOH (e.g. Breton et al., 2014). In Figure 6 it is visible that reasonable relationships between NO_x and SO_2 are found considering all PG values: correlation values, r_{SO_2,NO_x}, ranging from ~0.71 to ~0.35 and p-values < 0.0001. Interestingly, if the NO_x-SO_2 relationship is analysed for values of PG corresponding to PG > 150 V/m (not shown) the correlation values, r_{NO_x,SO_2}, are increased by up to 12 % and the opposite happens when considering PG < 150 V/m (not shown). An increase in the NO_x-SO_2 correlation is expected for polluted environments and this suggests that the condition PG > 150 V/m corresponds to heavier pollution than PG < 150 V/m. This confirms the possibility of using PG in urban environments as a proxy for pollution levels. Moreover, SO_2 is an important secondary particle precursor via oxidation in the atmosphere to form sulphuric acid, H_2SO_4, which is thought to play a significant role in the formation of PM (Kulmala et al., 2004; Zhang et al., 2004; Boy et al., 2005; Ristovski et al., 2010) and through Eq. 5 it will influence the PG. It should be noted that although

SO_2 emissions in Europe have been reduced significantly over recent decades (Verstreng et al., 2007), sulphate still contributes significantly to PM mass (Putaud et al., 2010). At the time of data collection, SO_2 emissions were much higher than present day levels and therefore may had a higher PM formation and consequently higher PG. This observation strengthens the possibility of using PG instead of PM when studying the relationship between particle and gaseous pollution, especially in the case of historical PG records, e.g, Aplin (2012). Coming back to Figure 6, it can be found:

- NW wind sector has the highest NO_x-SO_2 correlation, $r_{NO_x,SO_2} = 0.7093$, and the NO_x, SO_2 concentrations are ~150 ppb (some exceptions are observed);
- NE wind sector shows a lower NO_x-SO_2 correlation , $r_{NO_x,SO_2} = 0.4878$, and SO_2 concentrations reaching ~250 ppb, but the NO_x remaining lower than ~150 ppb;
- SE wind sector has a comparable behaviour with the NE sector, NO_x-SO_2 correlation $r_{NO_x,SO_2} = 0.4927$ and SO_2 < ~250 ppb and NO_x < ~150 ppb.
- SW wind sector has the lowest NO_x-SO_2 correlations, $r_{NO_x,SO_2} = 0.3473$ but the NO_x, SO_2 concentrations are ~150 ppb similar to the NW sector.

All the correlations have *p*-values < 0.0001. It can also be observed, that generically higher concentrations of NO_x and SO_2 correspond to high PG values, reinforcing again the possible role of PG as a proxy of pollution. The most important conclusion that can be drawn from Figure 6 is that the Eastern wind sectors, NE and SE, show evidence of an increase in PG (proportional to the PM number concentration) with SO_2 concentrations (that reach ~250 ppb) while the NO_x levels remain below ~150 ppb. Eastern wind sectors share the same characteristic of receiving land air masses that apparently have a more decisive rule in the SO_2, NO_x and PG relation, than the marine air masses that characterize Western wind sectors. This fact can be related with the fact that marine air masses transport small ions that tend to reduce the PG and the inverse happens with land air masses that bring dust and continental PM that tend to increase the PG.

5. Conclusions

This work presents a multidisciplinary study covering three different aspects in air pollution: PM, TG, and PG. Focus is given to the urban environment of the city of Lisbon (Portugal) in the late 1980s, when traffic was the main source of pollution within the city. The data analysed, though historic, constitutes a unique opportunity for studying simultaneous TG and PG. A reliable linear relation is found between TG concentration and PG which is justified by a formula developed to explain it. Two noteworthy results have been found: the constant of proportionally between TG

concentration and PM number concentration is estimated to be ~50 $cm^{-3}ppb^{-1}$, similar to experimental studies that measured PM directly; and evidence of a possible influence of SO_2 in PM formation for the SE wind sector is explored. These results are supportive of an indirect relationship between TG and PG mediated by PM. The present study considers PG measurements to relate TG with PM in an innovative way that could constitute a wide range of future applications regarding the use of Atmospheric Electricity as a tool for Air Quality monitoring.

Acknowledgments

Gratitude is expressed to Cláudia Serrano and Samuel Bárias for digitalizing the PG data recorded by Doctor Mário Figueira, who the authors also acknowledge. Discussions with Sérgio Pereira, Heitor Reis, Luísa Nogueira and Giles Harrison are recognized here. Researchers from the University of Évora acknowledge funding from the Portuguese Science and Technology Foundation (FCT) through the program Pest/OE/CTE/UI0078/2014. Researchers from the University of Bristol acknowledge funding from the Leverhulme Trust through grant RPG-2014-102 and Natural Environmental Research Council (NERC) through Grant No. NE/K01501X/1. Finally, the detailed review of the manuscript by one anonymous reviewer is gratefully acknowledged.

References

Anderson, R.V (1977). Atmospheric electricity in the real world - Useful applications of observations which are perturbed by local effects, in *Electrical Processes in Atmospheres*, edited by H. Dolezalek and R. Reiter, pp.87-99, Steinkopff, Darmstadt, Germany.

Aplin, K. (2012). Smoke emissions from industrial western Scotland in 1859 inferred from Lord Kelvin's atmospheric electricity measurements. Atmospheric Environment 50, 373.

Boy, M., Kulmala, M., Ruuskanen, T. M., Pihlatie, M., Reissell, A., Aalto, P. P., Keronen, P., Dal Maso, M., Hellen, H., Hakola, H., Jansson, R., Hanke, M., and F. Arnold (2005). Sulphuric acid closure and contribution to nucleation mode particle growth. Atmos. Chem. Phys. 5, 863–878.

Breton, M.L., Bacak, A., Muller, J.B.A., Xiao, P., Shallcross, B.M.A., Batt, R., Percival, C.J. et al. (2014). Simultaneous airborne nitric acid and formic acid measurements using a chemical ionization mass spectrometer around the UK: Analysis of primary and secondary production pathways. Atmospheric Environment 83, 166-175.

Chalmers, J.A., (1967). Atmospheric Electricity, 2nd edition (Section 2.7), Pergamon Press, Oxford.

Conceição, R., Silva, H.G., Melgão, M., Nicoll, K., Harrison, R.G. and Reis, A.H. (2015). Transport of the smoke plume from Chiado's fire in Lisbon (Portugal) sensed by atmospheric electric field measurements. Air Quality, Atmosphere & Health 8 (2015); Doi: 10.1007/s11869-015-0337-4.

Eyring, V., Isaksen, I.S.A., Berntsen, T., Collins, W.J., Corbett, J.J., Endresen, O., Grainger, R.G., Moldanova, J., Schlager, H. and Stevenson, D.S. (2010). Transport impacts on atmosphere and climate: Shipping. Atmospheric Environment 44, 4735-4771. Doi: 10.1016/j.atmosenv.2009.04.059

Fleming, J., Stern, R. and Yamartino, R.J. (2005). A new air quality regime classification scheme for O_3, NO_2, SO_2 and PM10 observations sites. Atmospheric Environment 39(33), 6121–6129. Doi: 10.1016/j.atmosenv.2005.06.039

Guo, Y., Barthakur, N.N., and Bhartendu, S. (1996a). The spectral relationships between atmospheric electrical conductivity and air pollution in urban conditions. Journal of Geophysical Research 101(D3), 6971-6977.

Guo, Y., Barthakur, N.N., and Bhartendu, S. (1996b). Using atmospheric electrical conductivity as an urban air pollution indicator. Journal of Geophysical Research 101(D4), 9197-9203.

Gunn, R. (1954). Diffusion charging of atmospheric droplets by ions and the resulting combination coefficients. Journal of Meteorology, 11, 339–347.

Harrison, R.G., Aplin, K.L. (2002). Mid-nineteenth century smoke concentrations near London, Atmospheric Environment 36, 4037.

Harrison, R.G., and Carslaw, K.S. (2003). Ion–aerosol–cloud processes in the lower atmosphere. Review of Geophysics, 41(3), 1012. Doi:10.1029/2002RG000114.

Harrison, R.G. (2004). The global atmospheric electrical circuit and climate. Surveys in Geophysics 25 (5-6), 441–484.

Harrison, R.G. (2006). Urban smoke concentrations at Kew, London, 1898-2004. Environment 40 (18), 3327-3332.

Hanrahan, G. (2010). Modelling of Pollutants in Complex Environmental Systems, Vol. 1, ILM Publications (UK).

Horowitz, L.W., Fiore, A.M., Milly, G.P., Cohen, R.C., Perring, A., Wooldridge, P.J., Hess, P.G., Emmons, L.K., Lamarque, J.-F. (2007), Observational constraints on the chemistry of isoprene nitrates over the eastern United States . J. Geophys. Res. Atmos. 112, D12S08.

Hoppel, W.A. (1985). Ion-aerosol Attachment Coefficients, Ion Depletion, and the Charge Distribution on aerosols. J. Geophys. Res. 90(D4), 5917-5923.

Jenkin, M.E., Clemitshaw, K.C. (2000). Ozone and other secondary photochemical pollutants: chemical processes governing their formation in the planetary boundary layer. Atmos. Environ. 34, 2499-2527.

Kirkby et al. (2016). Ion-induced nucleation of pure biogenic particles. Nature 533, 521. Doi:10.1038/nature17953

Kulmala, M., Kerminen, V.-M., Anttila, T., Laaksonen, A., and O'Dowd, C.D. (2004). Organic aerosol formation via sulphate cluster activation. J. Geophys. Res. 109, D04205. Doi: 10.1029/2003JD003961

Lanz, V.A., Prévôt, A.S.H., Alfarra, M.R., Weimer, S., Mohr, C., DeCarlo, P.F., Gianini, M.F.D., Hueglin, C., Schneider, J., Favez, O., D'Anna, B., George, C., and Baltensperger, U. (2010). Characterization of aerosol chemical composition with aerosol mass spectrometry in Central Europe: an overview. Atmos. Chem. Phys., 10, 10453–10471. Doi: 10.5194/acp-10-10453-2010

Longley, I.D., Inglis, D.W.F., Gallagher, M.W., Williams, P.I., Allan, J.D., and Coe, H. (2005). Using NO_x and CO monitoring data to indicate fine aerosol number concentrations and emission factors in three UK conurbations. Atmospheric Environment 39, 5157–5169.

Moller, D. (2010). Chemistry of the Climate System, Walter de Gruyter GmbH & Co, KG, Berlin/New York.

National Research Council - NRC (1991). Rethinking the ozone problem in urban and regional air pollution, Washington DC. National Academy Press.

Niemelä, J., Breuste, J., Elmqvist, T., Guntenspergen, G., James, P., and MacIntyre, N. (2011). Introduction. *in* J. Niemelä, J. Breuste, T. Elmqvist, G. Guntenspergen, P. James and N. MacIntyre (Editors) Urban Ecology: Patterns, Processes and Applications. Oxford Biology, Oxford (UK).

Pinto, D.M., Blande, J.D., Souza, S.R., Nerg, A.M., and Holopainen, J.K. (2010). Plant Volatile Organic Compounds (VOCs) in Ozone (O3) Polluted Atmospheres: The Ecological Effects. J. Chem. Ecol. 36, 22-34. Doi: 10.1007/s10886-009-9732-3

Putaud, J.-P., van Dingenen, R., Alastuey, A., Bauer, H., Birmili, W., Cyrys, J., Flentje, H., Fuzzi, S., Gehrig, R., Hansson, H.C., Harrison, R.M., Herrmann, H., Hitzenberger, R., Hüglin, C., Jones, A.M., Kasper-Giebl, A., Kiss, G., Kousa, A., Kuhlbusch, T.A.J., Loschau, G., Maenhaut, W., Molnar, A., Moreno, T., € Pekkanen, J., Perrino, C., Pitz, M., Puxbaum, H., Querol, X., Rodriguez, S., Salma, I., Schwarz, J., Smolik, J., Schneider, J., Spindler, G., ten Brink, H., Tursic, J., Viana, M., Wiedensohler, A., Raes, F., 2010. A European aerosol phenomenology - 3: physical and chemical characteristics of particulate matter from 60 rural, urban, and kerbside sites across Europe. Atmos. Environ. 44, 1308-1320. doi: 10.1016/j.atmosenv.2009.12.011

Ristovski, Z.D., Suni, T., Kulmala, M., Boy, M., Meyer, N.K., Duplissy, J., Turnipseed, A., Morawska, L., and Baltensperger, U. (2010). The role of sulphates and organic vapours in growth of newly formed particles in a eucalypt forest. Atmos. Chem. Phys. 10, 2919–2926. Doi: 10.5194/acp-10-2919-2010.

Scargle, J.D., (1982). Studies in astronomical time series analysis. II. Statistical aspects of spectral analysis of unevenly spaced data. The astronomical journal, 263:835-853.

Serrano, C., Reis, A.H., Rosa, R., Lucio, P.S. (2006). Influences of cosmic radiation, artificial radioactivity and aerosol concentration upon the fair-weather atmospheric electric field in Lisbon (1955-1991), Atmospheric Research, 81, 236.

Shah, J.J., Nagpal, T., and Brandon, C.J., (1997). Urban Air Quality Management Strategy in Asia Guidebook. The World Bank, Washington D.C.

Shoelson, B., (2001). www.mathworks.com/matlabcentral/fileexchange/993-lombscargle-m

Silva, H.G., Conceição, R., Melgão, M., Nicoll, K., Mendes, P.B., Tlemçani, M., Reis, A.H., and Harrison, R.G. (2014). Atmospheric electric field measurements in urban environment and the pollutant aerosol weekly dependence. Environment Research Letters 9, 114025. Doi:10.1088/1748-9326/9/11/114025.

Silva, H.G., Conceição, R., Wright, M.D., Matthews, J.C., Pereira, S.N., and Shallcross, D.E. (2015a). Aerosol hygroscopic growth and the dependence of atmospheric electric field measurements with relative humidity. Journal of Aerosol Science 85, 42-51. Doi: 10.1016/j.jaerosci.2015.03.003

Silva, H.G., Matthews, J.C., Conceição, R., Wright, M.D., Reis, A.H. and Shallcross, D.E. (2015b). Modulation of urban atmospheric electric field measurements with the wind direction in Lisbon (Portugal). J. Phys.: Conf. Ser. 646, 012013.

Tammet, H., Hõrrak, U., Laakso, L. and Kulmala, M. (2006). Factors of air ion balance in a coniferous forest according to measurements in Hyytiälä, Finland. Atmos. Chem. Phys. 6, 3377−3390.

Tasic, M., et al. (2006). Physic–Chemical characterization of PM10 and PM2.5 particles in the Belgrade urban area. Act Chemical Slovenia, 53, 401-405.

Tchepel, O. and Borrego, C. (2010) Frequency analysis of air quality time series for traffic related pollutants. J. Environ. Monit. 12, 544–50.

Verstreng, V., Myhre, G., Fagerli, H., Reis, S. and Tarrasón, L. (2007). Twenty-five years of continuous sulphur dioxide emission reduction in Europe. Atmos. Chem. Phys. 7, 3663-3681.

Wright, M.D., Holden, N.K., Shallcross, D.E., and Henshaw, D.L. (2014). Indoor and outdoor atmospheric ion mobility spectra, diurnal variation, and relationship with meteorological parameters. J. Geophys. Res. Atmos., 119. Doi: 10.1002/2013JD020956.

Zhang, Q., Stanier, C.O., Canagaratna, M.R., Jayne, J.T., Worsnop, D.R., Pandis, S.N., and Jimenez, J.L. (2004). Insights into the Chemistry of New Particle Formation and Growth Events in Pittsburgh Based on Aerosol Mass Spectrometry. Environ. Sci. Technol. 38, 4797-4809. Doi: 10.1021/es035417u

Table 1 – Mean, Median, Standard Deviation (Stan.), Skewness (Skew.), Kurtosis (Kur.), and number of hours (N.H.) for NO_x, SO_2, O_3 in the period between 1988 and 1990. The measurements are divided according to the wind direction in Portela: NW, NE, SE, and SW.

	NW			NE			SE			SW		
	NO_x	SO_2	O_3	NO_x	SO_2	O_3	NO_x	SO_2	O_3	NO_x	SO_2	O_3
Mean*	26.34	18.09	55.55	39.97	74.30	42.03	25.85	43.52	42.48	21.39	17.33	42.00
Median*	16.00	10.48	39.24	31.00	57.64	34.90	21.00	26.20	33.35	16.00	10.48	37.28
Stan.*	32.95	21.65	116.87	30.76	61.73	31.07	20.07	48.65	41.45	20.34	22.41	26.05
Skew.	3.59	3.73	8.64	2.56	2.10	3.72	2.45	2.61	6.99	3.26	4.79	3.58
Kurt.	18.98	24.78	8.64	14.56	10.49	22.57	11.54	11.90	82.34	19.41	37.93	27.15
N.H.	975	971	954	913	992	969	468	482	474	744	738	752

* These parameters have units in ppb.

Table 2 – Results from fitting the model to the PG in the northern wind sectors: background PM number concentration, $Z_{0,X}$; constant of proportionality between TG and the PMs number concentration, $y_{[X]}$. The goodness of the fit is also given, r^2. It is assumed that particle radius is R_a = 0.1 μm.

	NW			NE			SE			SW		
	NO_x	SO_2	O_3	NO_x	SO_2	O_3	NO_x	SO_2	O_3	NO_x	SO_2	O_3
$Z_{0,X}$*	3360	3350	2642	3563	3997	3585	3844	5134	3825	4331	4802	3589
$y_{[X]}$**	27.38	45.73	35.14	55.40	21.32	47.91	82.61	21.77	59.53	33.31	38.39	46.22
R^2	0.9992	0.998	0.9999	0.9994	0.9999	0.999	0.95	0.998	0.998	0.99	0.92	0.996

*These parameters have units in cm^{-3} and estimated errors < 1 cm^{-3}. **These parameters have units in $cm^{-3}ppb^{-1}$ and uncertainties < 0.01 $cm^{-3}ppb^{-1}$.

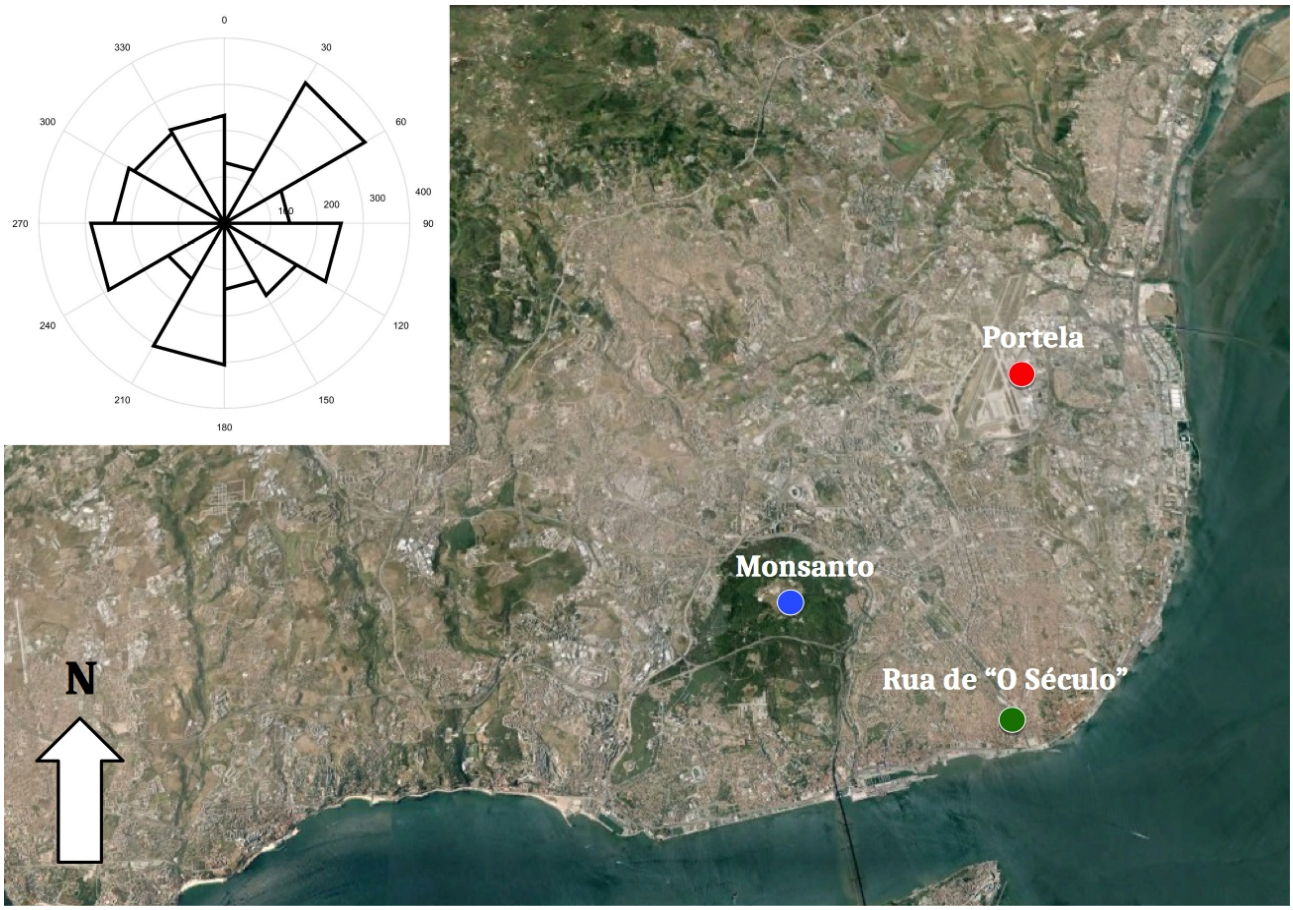

Figure 1 – Location of the Portela meteorological station (red dot) where Potential Gradient and Wind measurements were made, Rua de "O Século" (green dot) where Trace Gases measurements were made and Monsanto (blue pin) are marked. Inset shows the wind rose with a 30º binning for winds having simultaneous measurements of PG, NO_x, SO_2, and O_3.

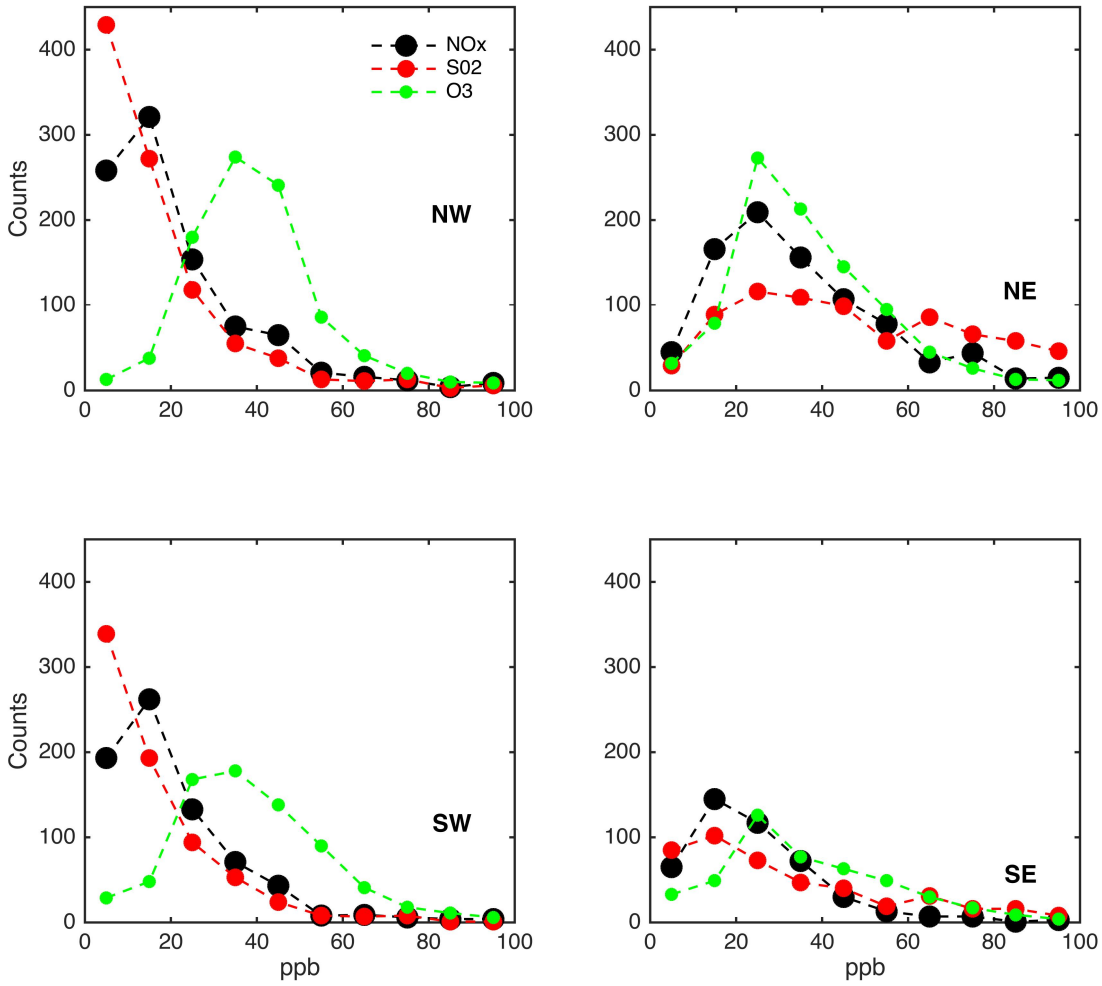

Figure 2 – Distributions of the hourly values of NO_x (black), SO_2 (red) and O_3 (green) for the four wind sectors: NW, NE, SE, and SW. Counts signifies total number of occurrences in a given bin.

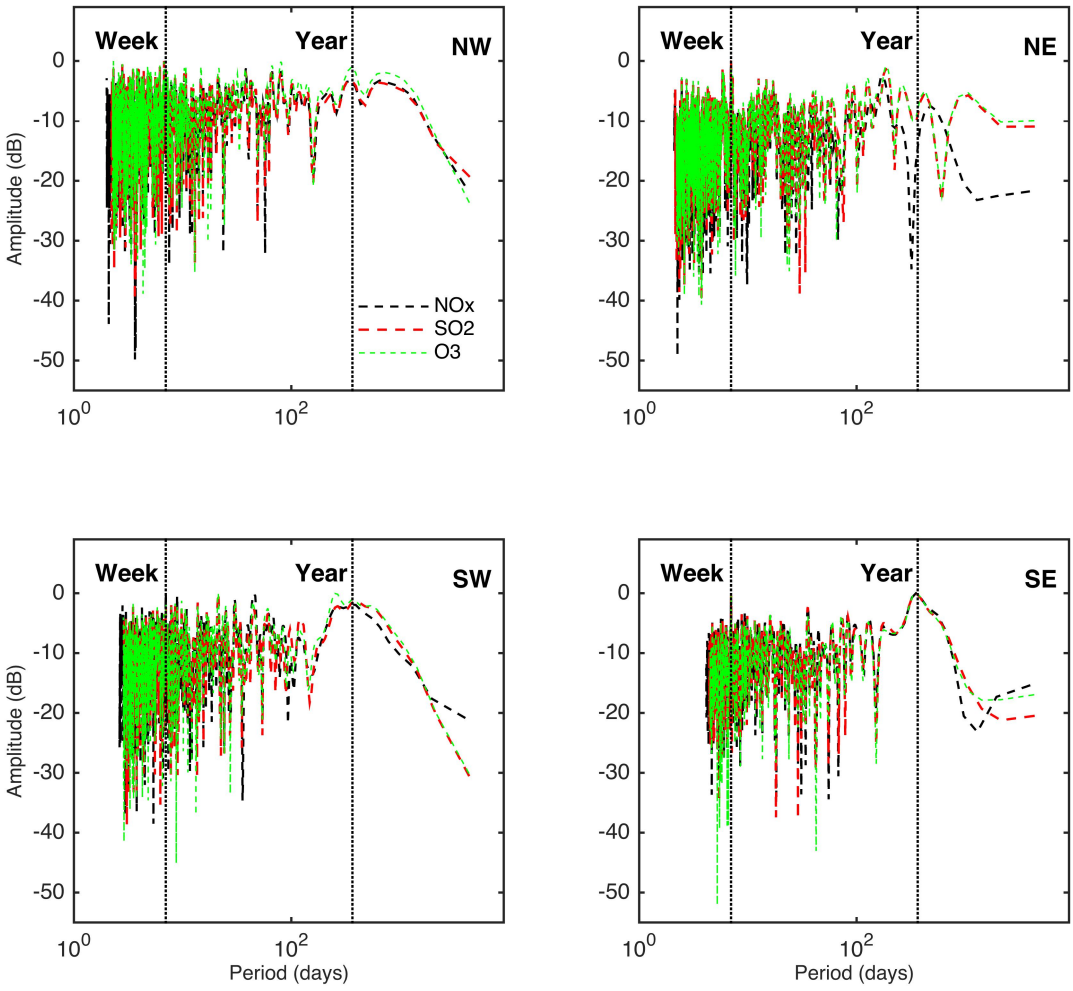

Figure 3 – Lomb-Scargle Periodogram for NO_x (black), SO_2 (red) and O_3 (green) corresponding to the four wind sectors. The following parameters were used *hifac* = 1 (that defines the frequency limit as *hifac* times the average Nyquist frequency), *ofac* = 4 (oversampling factor). Marked by the left vertical dashed line is the weekly cycle while the right vertical dashed line denotes the annual

cycle.

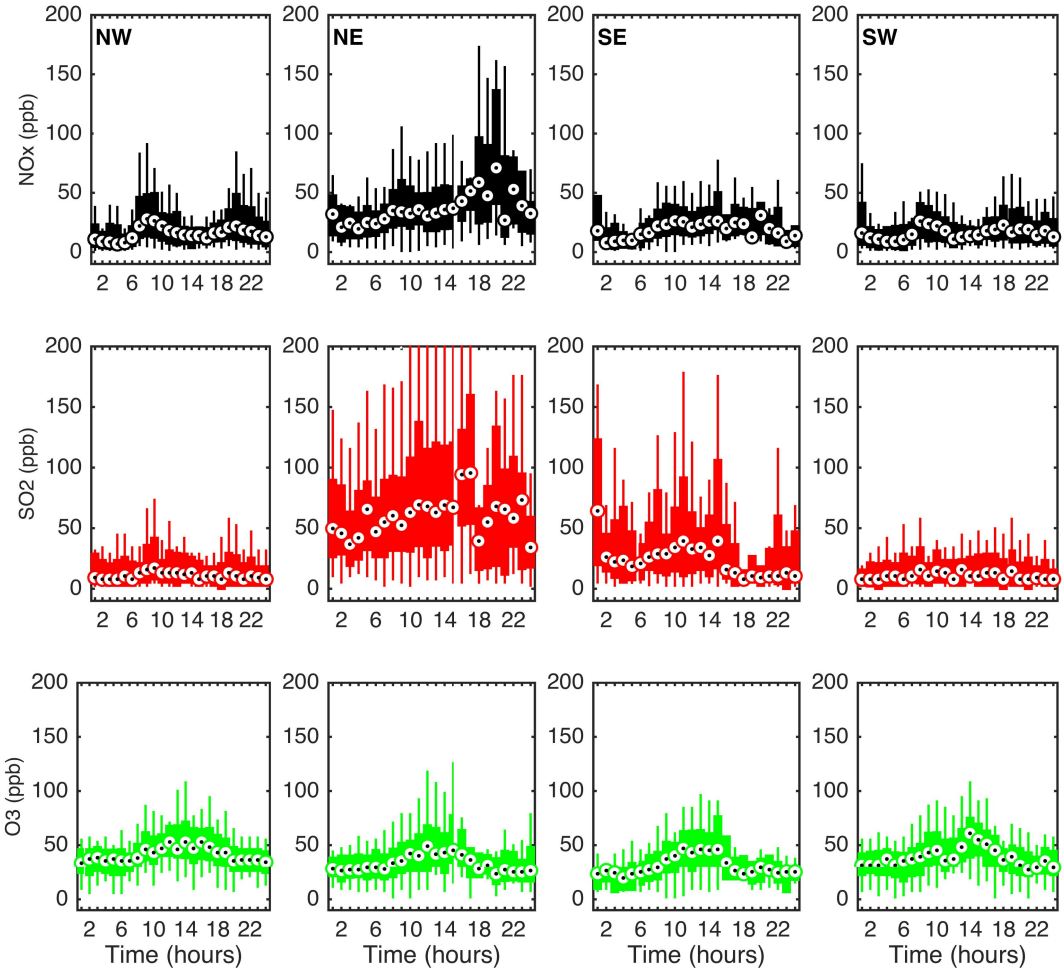

Figure 4 – Diurnal variation of hourly NO_x, SO_2, and O_3 values in a boxplot representation, respectively, in the first, second and third rows. The four wind sectors are considered: NW, NE, SE, and SW, respectively in the first, second, third and fourth columns. On each box, the central dot is the median, the limits of the box are the 25th (first quartile, q_1) and 75th (third quartile, q_3) percentiles and the whiskers (solid lines) extend to the most extreme data points not considered outliers. Maximum whisker length (w) is set to 1.5 and outliers are defined to be larger than $q_3+w(q_3-q_1)$ or smaller than $q_1-w(q_3-q_1)$.

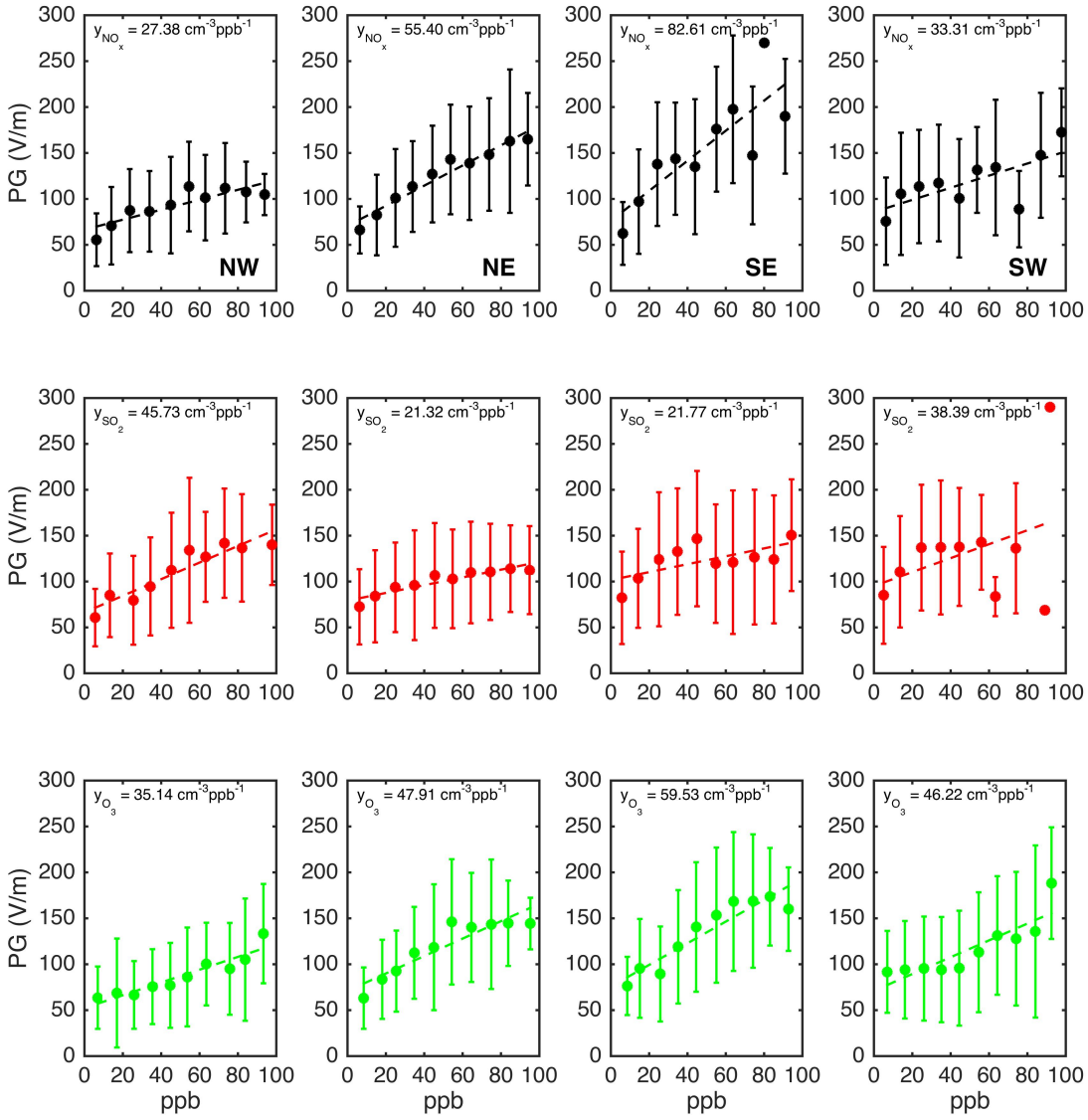

Figure 5 – The fits of the model in Equation 8 to the four wind sectors for NO_x (black, in the first line), SO_2 (red, in the second line) and O_3 (green, in the third line). The error bars represent the standard-deviation for each bin of data considered.

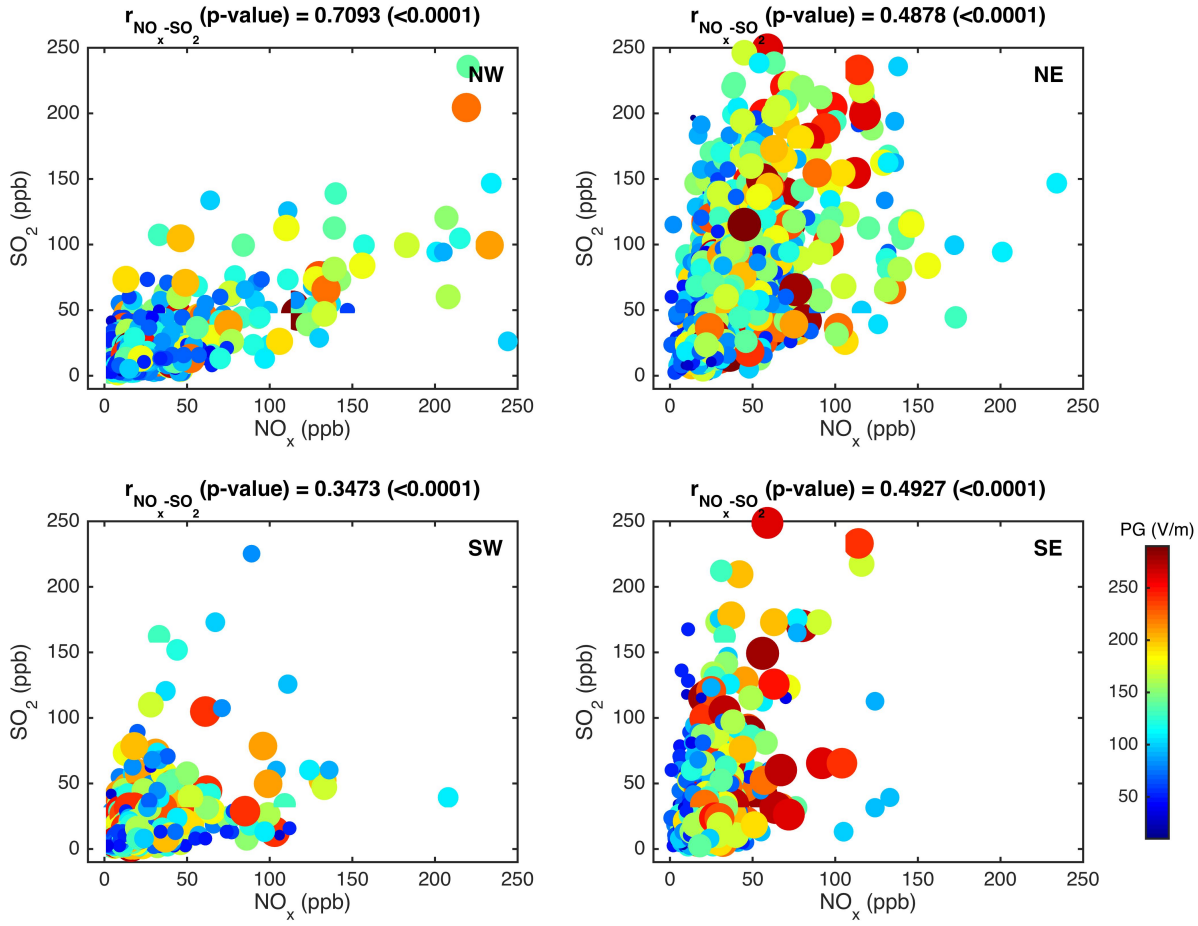

Figure 6 – Scatter plots of SO_2 as a function of NO_x with the corresponding values of PG represented as a colour gradient, for each wind sector: NW, NE, SE, and SW.